Vol 13 No 12, December 2004
1009-1963/2004/13(12)/2174-07

Chinese Physics

© 2004 Chin. Phys. Soc.
and IOP Publishing Ltd

Numerical simulation of chemical processes in atmospheric plasmas

Ouyang Jian-Ming(欧阳建明)[a)b)†], Guo Wei(郭 伟)[b)],
Wang Long(王 龙)[b)], and Shao Fu-Qiu(邵福球)[a)]

[a)] *National University of Defence Science and Technology, Changsha* 410073, *China*

[b)] *Institute of Physics, Chinese Academy of Sciences, Beijing* 100080, *China*

(Received 25 May 2004; revised manuscript received 24 June 2004)

A model is built to study chemical processes in atmospheric plasmas at low altitude (high pressure) and at high altitude (low pressure). The plasma lifetime and the temporal evolution of the main charged species are presented. The electron number density does not strictly obey the exponential damping law in a long period. The heavy charged species are dominant at low altitude in comparison with the light species at high altitude. Some species of small amount in natural air play an important role in the processes.

Keywords: atmospheric plasma, chemical processes, lifetime
PACC: 9410F, 5265, 7220J, 8670G

1. Introduction

The interest in the study of atmospheric discharge has been extraordinary in the last decade because of its low cost and convenient operation, as the gas discharge does not need vacuum equipment. Microwave plasma, RF plasma gun, DBD (dielectric barrier discharge) and surface discharge, which have been developed recently, are widely used in the fields such as chemical industry, material science, medical attendance and national defense.

Atmospheric discharges usually operate in two regimes. One is the discharge in an open atmosphere environment, near the earth surface (or in the horizon plane; the pressure is 10^5Pa) or at high altitude (low pressure). The other is the discharge in closed vessels with air as working gas. The former will be discussed in this paper.

Air is a complex working medium of discharge. Gravitational separation does not happen below 80km, where the turbulent diffusion is dominant in air and its composition is almost constant: that is, nitrogen 78%, oxygen 21%, argon 1%, vapour 0–4% and a small amount of CO_2. At high altitude, the solar radiation generates some excited states of oxygen molecule, oxygen atoms, ozone molecules and several species of nitrogen compounds. And their number densities change with altitude, season, time and latitude.

When air at atmospheric pressure is ionized, the physicochemical processes are very complex. The physical processes include excitation, ionization, attachment, recombination, detachment, charge exchange and so on. The chemical processes include all species of redox reactions. All these processes complicate the temporal evolutions of the components of the air. The generation of negative ions is a particularly important characteristic of atmospheric plasma in comparison with the usual lab plasmas. In air, the electrons are attached to neutral oxygen molecules very quickly, through two-body or three-body attachments once the electrons are generated. Negative oxygen ions produced can react with neutral species to form other species of negative ions. So the negative-ion number densities can be large in atmospheric plasma. The generation processes of gas-discharge plasmas are similar to the ionization processes in the ionosphere. The plasmas, in which negative ions are dominant, are defined as electronegative plasmas, and have many special characteristics.

Physicochemical processes of gas-discharge in atmospheric pressure are concerned in many related

†E-mail: oyjm@aphy.iphy.ac.cn. Tel:010-82649131-17.

fields. In some applications, such as plasma radio technology, and ionospheric artificial irregularities, electrons would be the primary conducting components, which are useful to absorb or reflect electromagnetic waves. Then the key parameter is the lifetime of electrons in the plasma. In addition, oxygen atom is the most important component in the technique of plasma sterilization. As for the plasma chemical industry, we care for the lifetime of all species of radicals of atoms or molecules. Because air components, especially some components of small amount, are difficult to be controlled and measured, but play important roles in experiments, numerical simulation becomes a convenient method to study the processes.

Our work is based on the work of Vidmar.[1] He simulated the lifetimes of electrons at various altitudes and with different initial electron number densities during ionization processes, obtaining the plasma lifetime curves as functions of altitude, and found that at low altitude three-body reactions determine the plasma lifetimes, while two-body reactions are dominant at high altitude. The temporal evolutions of various components were not presented in his papers, but constitute the object of our present research.

An atmospheric chemical code has been compiled in the present work, and calculation results are presented for both atmospheric and low pressures.

2. The model and numerical simulation

The numerical calculation in this paper is zero-dimensional. It includes ionization, attachment, and other physical processes as well as the main chemical reactions, but ignores spatial processes such as diffusion and flow. As the initial condition, electrons and positive ions with the same number are added. Then the temporal evolutions of various components are monitored during the simulation; some of them belong to the components of natural gas, and some are generated during the chemical reactions. In other words, the process studied is a pulsed ionization with very short ionization reaction period. We do not care about the ionization means (discharge or microwaves) but focus only on the processes after the electron generation.

2.1. Atmospheric chemical reactions

The atmospheric chemical reactants include some charged species, which complicate the processes. We can only study some main reactions, and are interested in the reactions involving the ions, because these reactions determine the number density evolution of charged species and the plasma lifetime. At low altitude, three-body attachment to oxygen (reaction (1)) dominates the deionization process, and three-body attachment is proportional to the square of the density of oxygen molecules:

$$O_2 + e + O_2 \longrightarrow O_2^- + O_2. \quad (1)$$

As the concentration of oxygen diminishes with increasing altitude, two-body attachment and recombination processes begin to override the three-body attachment to oxygen. These processes include dissociative attachment with oxygen (reaction (2)) and ozone (reaction (3)), and dissociative recombination with positive ions (reaction (4)) as follows:

$$e + O_2 \rightarrow O^- + O, \quad (2)$$

$$e + O_3 \rightarrow O^- + O_2, \quad (3)$$

$$O_2^+ + e \rightarrow O + O. \quad (4)$$

Because attachment depends on the concentration of oxygen and ozone but recombination does not, recombination with positive ions is the dominant loss mechanism at high altitude.

2.2. The model

The initial electrons are generated by air ionization in our model, and the same number densities of positive ions (O_2^+, N_2^+) are added. The ratio of the oxygen to nitrogen ions is the same as in natural air. The initial number densities of other neutral species are found from some atmospheric chemical papers.[2,3]

Thirty-four species of reactants are considered in our model, as shown in Table 1, including neutral species, positive species (positive ions, hydrated positive ions) and negative species (electron, negative ions, hydrated negative ions), and 134 reactions are considered, including attachment, recombination, detachment, charge exchange and so on.

Table 1. The main reactants.

Neutral species	Positive species	Negative species
O,O_2, O_3, N, N_2,	O^+, O_2^+, N_2^+, N_4^+, NO^+,	e, O^-, O_2^-, O_3^-, O_4^-,
NO, NO_2, CO_2,	O_4^+, H_2O^+, H_3O^+,	CO_3^-, CO_4^-,
H_2O, H, H_2,	$O_2^+ \bullet H_2O$, $H_3O^+ \bullet OH$,	$O_2^- \bullet H_2O$, $CO_3^- \bullet H_2O$,
OH, He	$H_3O^+ \bullet H_2O$	$CO_4^- \bullet H_2O$

The reacting charts for the main positive charge reacting and negative charge reacting near the surface are shown in Figs.1 and 2, respectively. The main reactions of different periods are shown in the figures with bold lines.

At high altitude (low pressure), the reacting charts are different from that at low altitude, as shown in Figs.3 and 4. Light species, such as O^-, O_2^-, NO^+, are important at high altitude in comparison with heavy positive species, such as CO_4^-, CO_4^-, $H_3O^+ \bullet H_2O$, at low altitude.

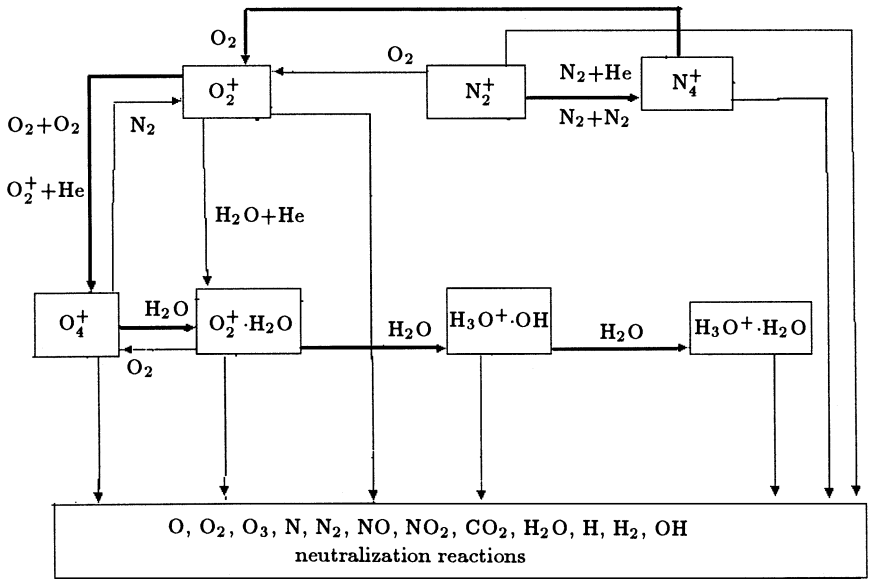


Fig.1. Reacting chart of the main positive ions at low altitude. (The arrows are the reacting directions, and the species near the arrows are reactants. The plus sign means the reaction is a multi-body reaction. The species in the biggest block are the reactants of the neutralization reactions).

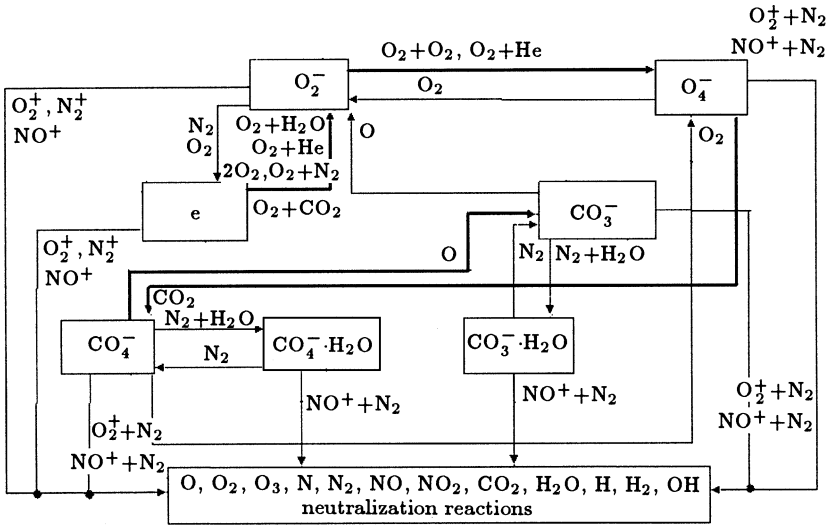


Fig.2. Reacting chart of the main negative ions at low altitude.

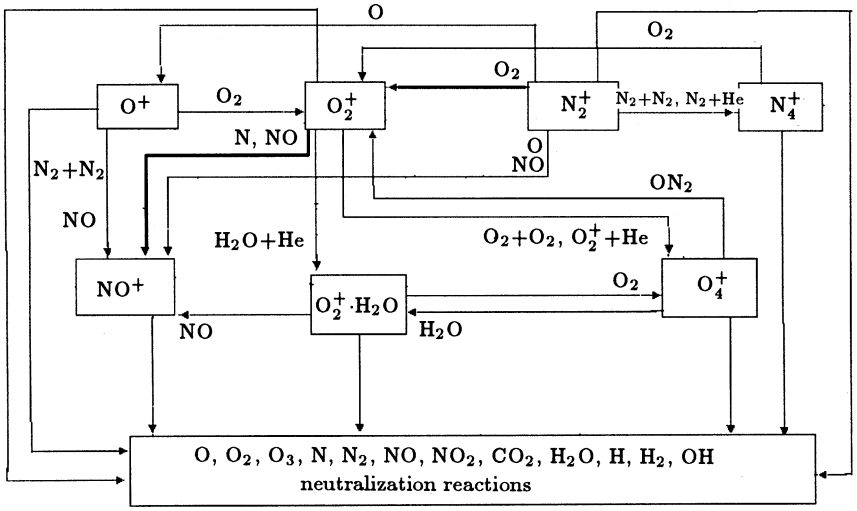


Fig.3. Reacting chart of the main positive ions at high altitude.

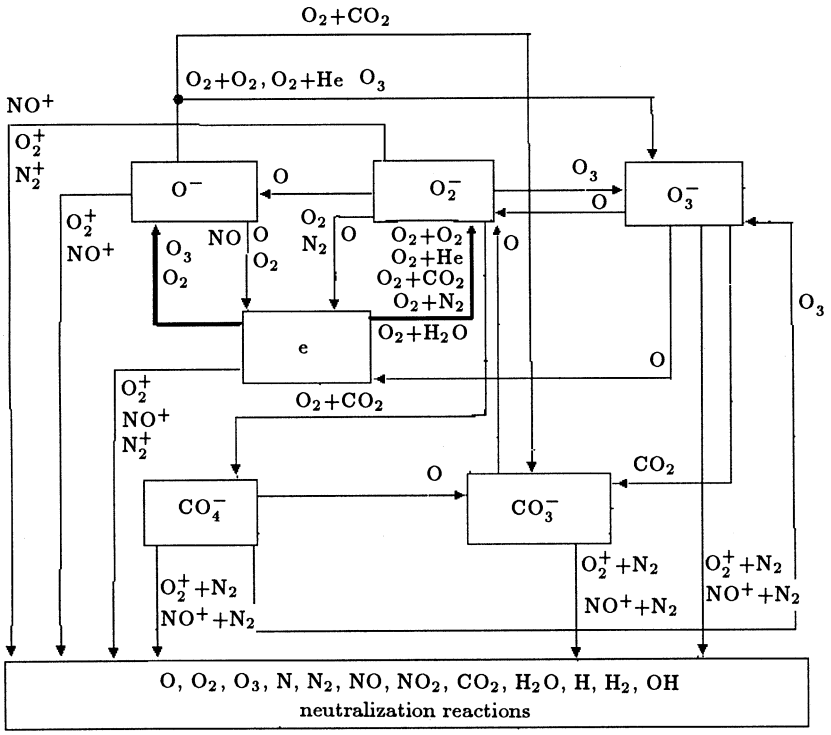


Fig.4. Reacting chart of the main negative ions at high altitude.

2.3. Numerical simulation method

In our model the reaction rate equations are as follows:[1]

$$\frac{\mathrm{d}y_i}{\mathrm{d}t} = f_i(t, y_1, y_2, \ldots, y_{34}) \quad i = 1, 2, \ldots, 34, \qquad (5)$$

$$f_i = y_i \sum_{j=1}^{34} n_{ij} k_{ij} y_j + y_i \sum_{m=1}^{34} \sum_{j=1}^{34} n_{ijm} k_{ijm} y_j y_m, \qquad (6)$$

where y_i denotes the number density of the ith species and f_i is a function involving the rate coefficient for reactions among the ith, jth, and mth species. The terms k_{ij} and k_{ijm} refer to two-body and three-body reaction rates, respectively. The term n_{ij} or n_{ijm} is the integer number of the ith species produced or consumed per reaction event, and is positive if the ith species is produced, and negative if it is consumed.

The Runge–Kutta method[4] is used to solve the constant coefficient nonlinear equations, because the degree of the accuracy of high-order Runge–Kutta method is very high. Considering the simulating time,

we take the fourth-order Runge–Kutta method, with a high degree of accuracy and short time of simulation.

3. Result of numerical simulation and analysis

3.1. Initial condition and rate coefficient

The initial electron number density near the surface is set to be $10^{13}/\mathrm{cm}^3$, and the initial number density of O_2^+ is $2.6\times10^{12}/\mathrm{cm}^3$, N_2^+ $7.4\times10^{12}/\mathrm{cm}^3$ in our calculation. Considering there would be large number densities of O_2^+ and water, $O_2^+\bullet H_2O$ number density is set to be $10^6/\mathrm{cm}^3$. The initial electron number density is $10^{12}/\mathrm{cm}^3$, O_2^+ $2.6\times10^{11}/\mathrm{cm}^3$, N_2^+ $7.4\times10^{11}/\mathrm{cm}^3$, and $O_2^+\bullet H_2O$ $10^5/\mathrm{cm}^3$ at 60km altitude.

Some reaction rate coefficients are functions of atmospheric temperature and electron temperature. Atmospheric temperature is set to be 291K near the surface, 253K at 60km altitude,[3] and electron temperature is 2eV, or about 23200K. The pressure is 10^5Pa near the surface, and 20Pa at 60km altitude. The step length t_0 in our simulation is 10^{-25}s in the first phase of the calculation. Such a small step length is necessary to avoid overflow as the number density of electrons is large in this phase. As the number density decreases the step length increases automatically.

3.2. Results and discussions

Figure 5 shows in logarithmic coordinates the temporal evolutions of electron number density and the total negative charges near the surface. The solid line shows the electron number density, and the dashed line is the total negative charges. Figure 6 shows the temporal evolution of electrons at 60km altitude. Electron number density is greater than that of other negative species and exceeds the total number of the latter by several orders of magnitude at the altitude. So the temporal evolution of the total negative charges is practically the same as that of the electron number density.

As shown in Fig.5, the electron lifetime is 1.95×10^{-8}s, close to Vidmar's[5] result of about 1×10^{-8}s. The lifetime of the total negative charges is 10^{-7}s, longer than the electron lifetime by about one order of magnitude. The main reason of the difference in lifetime is that the negative charges transfer from electrons to other negative species. As shown in Fig.7, negative charges transfer to O_2^- within the initial one microsecond.

As shown in Fig.5, the electron number density exponentially damps before 0.5μs. The above-mentioned lifetime was calculated within that time period. But it no longer obeys the exponential damping law from 0.5μs to 20μs. Two reasons give rise to this: (i) electron detachment generates new electrons; (ii) as shown in Fig.8, as the number densities of the carbon-bearing negative ions increase to a maximum in the submicrosecond interval, some charges of these negative ions transfer into the carbon-free negative ions and electrons. So during this period the temporal evolution of every carbon-free negative species has an inflection. Electron number density is between $10^6/\mathrm{cm}^3$ and $10^4/\mathrm{cm}^3$ in this range of time.

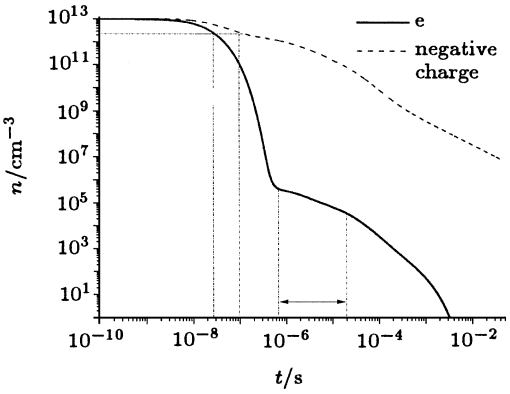


Fig.5. Number density temporal evolutions of electron and the total negative charges near the surface.

The temporal evolution of the total negative charges does not obey the exponential damping law also in a longer period because of charge exchanges of the negative species, and can be shown to be inversely proportional to the square root of time after 10μs.

As shown in Fig.6, the electron lifetime at 60km altitude is 5.7×10^{-5}s, longer than that near the surface by three orders of magnitude, and is longer than Vidmar's[5] by about one order of magnitude. And the electron density does not obey the exponential damping law after 1ms. The electron number density is about 10^9–$10^{11}/\mathrm{cm}^3$ from 0.5ms to 5ms.

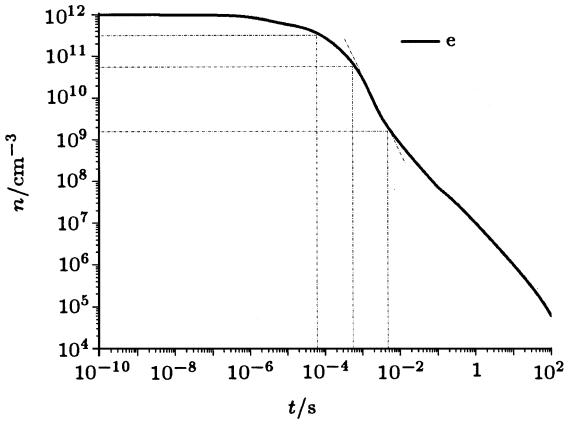


Fig.6. Electron temporal evolution at 60km altitude.

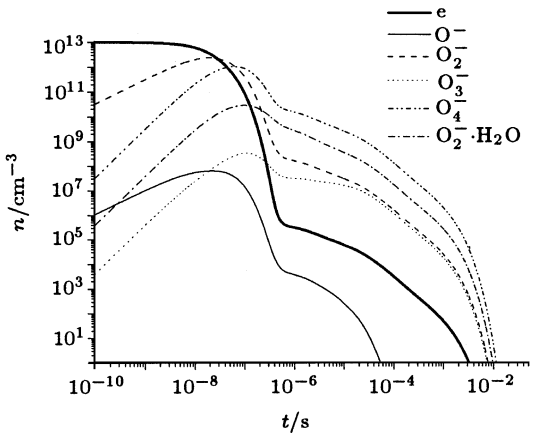


Fig.7. Carbon-free negative species temporal evolutions near the surface.

Figures 7 and 8 show respectively the number density temporal evolutions of carbon-free and carbon-bearing negative ions near the surface. As shown in the two figures, the dominant negative species devolution is as follows:

$$\mathrm{e} \longrightarrow \mathrm{O}_2^- \longrightarrow \mathrm{O}_4^- \longrightarrow \mathrm{CO}_4^- \longrightarrow \mathrm{CO}_3^-,$$

CO_4^- keeps in the longest time of about 1ms as the main negative ion species. After 20μs the number density of $CO_4^- \bullet H_2O$ is nearly equal with CO_4^-. Evolution of every carbon-free negative ion has an inflection in the submicrosecond interval. Within the initial one microsecond, charges transfer from carbon-free negative species to carbon-bearing ions through charge exchanges, and the latter increase to their maximum in the submicrosecond interval. Then charges transfer back to carbon-free negative species. So carbon-free negative species decrease more slowly during this period, and the inflections come into being. Only CO_3^- and $CO_3^- \bullet H_2O$ exist with large amounts in our simulation after 1ms. The number density of CO_3^- is $5 \times 10^7/\mathrm{cm}^3$ in 50ms, and $CO_3^- \bullet H_2O$ is less than CO_3^- by one order of magnitude.

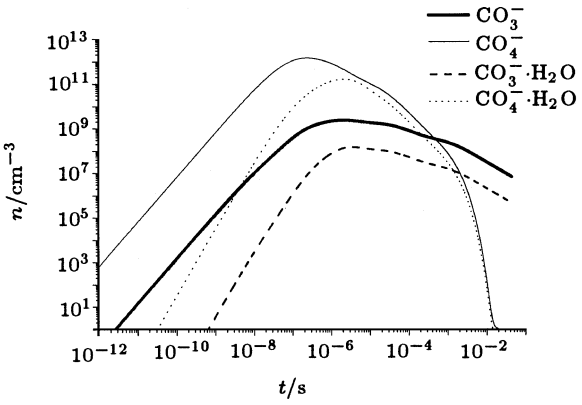


Fig.8. Carbon-bearing negative species temporal evolutions near the surface.

Figure 9 shows the number density temporal evolutions of the main negative species at 60km altitude. As shown in the figure, electron number density is greater than the other negative species or their totals by several orders of magnitude. Light negative ions (O^- and O_2^-) are dominant at this altitude, opposite to heavy negative species (CO_3^-, CO_4^- and their hydrates) near the surface. Their number densities reach the maximum of about 10^6–$10^7/\mathrm{cm}^3$ in the range of 10^{-6}–10^{-3}s. Other negative ions reach their maximum values in the range of 10^{-3}–10^{-2}s.

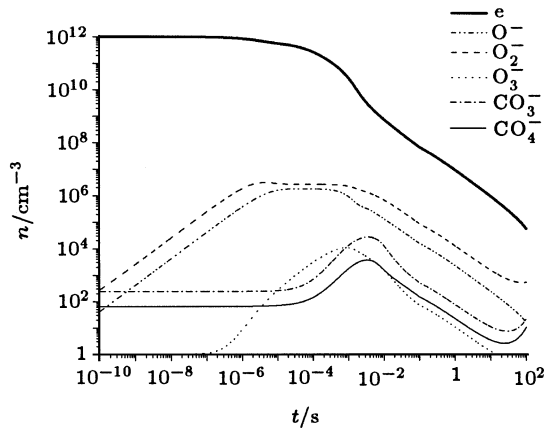


Fig.9. Main negative species temporal evolution at 60km altitude.

Figures 10 and 11 show the temporal evolutions of the main positive ions near the surface and at 60km altitude, respectively. As shown in the figures, the number density evolution of the total positive charges is the same as that of the total negative charges. The dominant positive species near the surface devolution is as follows:

$$N_2^+ \longrightarrow N_4^+ \longrightarrow O_2^+ \longrightarrow O_4^+ \longrightarrow H_3O^+ \bullet H_2O,$$

O_4^+ remains for the longest time of about 0.1ms as the main positive species. The heaviest positive species, $H_3O^+ \bullet H_2O$, is dominant at the end. N_2^+ number density exponentially damps to near $1/cm^3$ within the initial 10^{-9}s. The positive charges transfer into N_4^+ and O_2^+. Then the charges of N_4^+ transfer to O_2^+. O_2^+ number density increases to a maximum of about $10^{13}/cm^3$ at about 10^{-9}s. The number densities of the five positive species, $O_2^+ \bullet H_2O$, $H_3O^+ \bullet OH$, $H_3O^+ \bullet H_2O$, O_2^+ and O_4^+ are all in the range of 10^9–$10^{10}/cm^3$ at about 0.1ms, and $H_3O^+ \bullet H_2O$ begins to override O_4^+.

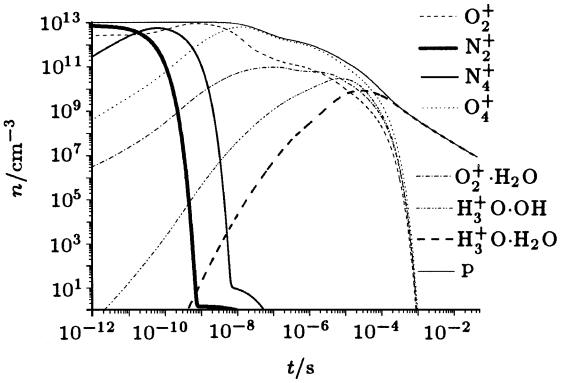


Fig.10. Main positive species temporal evolution near the surface.

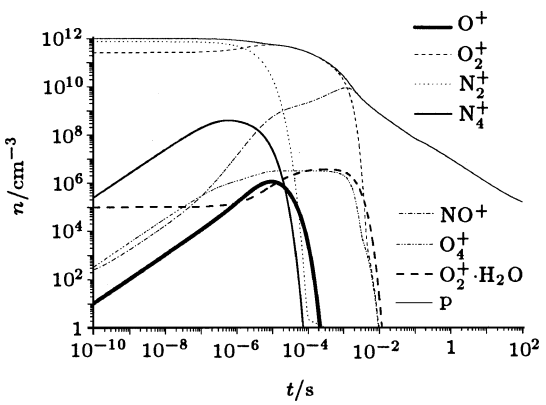


Fig.11. Main positive species temporal evolution at 60km altitude.

The number density temporal evolutions of main positive species at 60km altitude are different from those near the surface. The main positive species evolution is as follows:

$$N_2^+ \longrightarrow O_2^+ \longrightarrow NO^+,$$

N_2^+ number density exponentially damps within the initial one millisecond. O_2^+ number density increases to a maximum of about $10^{12}/cm^3$ in the submillisecond interval. NO^+ number density increases to a maximum of $10^{10}/cm^3$ at 10ms. NO^+ begins to dominate O_2^+ at this time.

4. Conclusions

Air is a very complex chemical system, and studying its chemical processes is very useful to some applications, such as plasma ratio technology, low-pressure atmospheric plasma, ionospheric artificial modifications and so on. A model has been built to simulate the chemical processes near the surface (the pressure is 10^5Pa and air temperature is 291K) and at high altitude (60km in our simulation, 20Pa, 253K). The temporal evolutions of the main charged components are presented.

(i) The electron lifetime at high altitude is longer than that near the surface. The number density of negative ions begin to override the electrons soon at low altitude, but electrons are dominant from beginning to end at high altitude. Electrons do not obey the exponential damping law in a longer period, as shown in Figs.5 and 6. So electron number density temporal evolutions are more useful than lifetime data from the application aspect. Especially, it is always expected there will be a need to generate and sustain a high electron number density in atmosphere in some application fields such as artificial plasma layer radio, and this requires high averaged heating power. The usual way to generate electrons is pulsed RF discharge. Proper choice of the repetition frequency and pulse width of the RF waves would increase the ionization efficiency.

(ii) Numerical simulation shows that the main charged species near the surface are heavy species such as CO_4^-, CO_3^-, $CO_3^- \bullet H_2O$ and $H_3O^+H_2O$, as opposed to light species, such as e, O^-, O_2^- and NO^+ at high altitude (low pressure). Most of the main charged species do not obey the exponential damping law, and they can keep a high density for a long period.Tthe

species of small amount in neutral air play an important role in the processes. They can be the dominant charged species in some periods. Therefore, a small amount of species artificially introduced can control the process and lengthen the lifetime of the electrons or other ions and radicals for certain application purposes.

References

[1] Vidmar R J 1990 *SRI Final Report For AFOSR/NP Contract F49620-85-K0013*

[2] Brasseur G and Solomon S 1984 *Aeronomy of the Middle Atmosphere* (Boston, MA: Reidel)

[3] Heicklen J 1976 *Atmospheric Chemistry* (New York: Academic)

[4] Zhang Y H, Xi M C and Cheng C S 2000 *Numerical Method and Algorithms* (Beijing: Science Press) p153 (in Chinese)

[5] Vidmar R J 1990 *IEEE Trans. Plasma Sci.* **18** 733